Romanian Reports in Physics, Vol. 66, No. 2, P. 472–480, 2014

PLASMA PHYSICS

CONVOLUTION BASED MODEL OF BREAKDOWN VOLTAGE DISTRIBUTIONS IN NEON AT 1.33 mbar WITH CORONA APPEARANCE IN PRE-BREAKDOWN REGIME*

M.K. RADOVIĆ[1], Č.A. MALUCKOV[2], J.P. KARAMARKOVIĆ[3], S.A. RANČEV[1], S.D. MITIĆ[4]

[1] University of Niš, Faculty of Science and Mathematics, Department of Physics, 18001 Niš, Serbia,
E-mail: mkradovic@yunis.ni.ac.rs; E-mail: sasa.rancev@gmail.com
[2] University of Belgrade, Technical Faculty in Bor, 19210 Bor, Serbia,
E-mail: cmaluckov@tf.bor.ac.rs
[3] University of Niš, Faculty of Civil Engineering and Architecture, 18000 Niš, Serbia,
E-mail: fizika@gaf.ni.ac.rs
[4] "Max Plank" Institute for Extraterrestrial Physics, Postfach 1213, 85748 Garching, Germany,
E-mail: smitic@verat.net

Received September 14, 2012

Abstract. Experimental and theoretical breakdown voltage distributions in the gas diode filled with neon are presented in this paper. Linearly increasing voltage was applied to the diode with the voltage increasing ratio k in range from 0.3 V/s up to 26 kV/s. The theoretical model - statistical model is based on convolution of the statistical and formative time delay. The statistical model nicely reproduce the experimentally determined the breakdown voltage distributions, especially good for description of the "left tail" of breakdown distributions which are not properly interpreted before. The presence of the "left tail" of the distributions indicates that the formative time delay distribution cannot be neglected in theoretical description of the breakdown voltage distributions.

Key words: breakdown voltage distribution, statistical convolution model, electrical breakdown, Neon.

1. INTRODUCTION

Electrical breakdown in gases represents the transition of gases from dielectric to conducting state. The voltage value at which the breakdown occurs is declared as breakdown voltage U_B [1]. Investigation of electrical breakdown in gases is important for describing processes and characteristics of gases as well as their practical applications [2–4]. The electrical breakdown of gases can be treated

* Paper presented at the 8th General Conference of Balkan Physical Union, July 5–7, 2012, Constanta, Romania.

as a macroscopic event with a stochastic nature which is the consequence of the statistical behavior of the processes leading to it. It was early described by Zuber and von Laue (1925) [5,6] and later the statistical theory of the electrical breakdown was developed by Loeb (1948) [7] and Wijsman (1949) [8]. The theory is established on the presumption of the Townsend breakdown mechanism [9]. For small pressure and small overvoltages, when the influence of the space charge can be neglected, Townsend theory is applicable with the breakdown criterion:

$$\gamma\left[\exp\left(\int_0^d \alpha \mathrm{d}x\right) - 1\right] = 1, \tag{1}$$

where α is the primary ionization coefficient and γ is the effective secondary ionization coefficient (this coefficient includes all secondary processes). The lowest voltage value for which this criterion is fulfilled is defined as a static breakdown voltage U_S.

It is widely accepted that the electrical breakdown mechanism in gases can be considered as a combination of two distinct processes. First of them corresponds to the physical events which leads to creation of an initial free electron. Time needed to electron appearance is statistical time delay t_S, characterized with the exponential distribution [1]. Second process is the actual process of impact ionization and carrier multiplication in the gas. This is associated to the breakdown formative time delay t_F, with the Gaussian distribution [10, 11]. Following this analysis, the electrical breakdown time delay t_D consists of the statistical time delay and the breakdown formative time t_F , $t_D = t_S + t_F$ [1].

The formative time delay can be expressed as the sum of three time stages [12]. The first stage begins with appearance of initial electron and ends when the threshold value of voltage is reached. The second stage corresponds to the duration of the avalanche process, which creates a conducting channel between the anode and cathode. During the final stage, the subsequent increase of the conductivity and current in the plasma channel appear. This results in an observable decrease in the discharge voltage [12].

However, in some publications the investigations of prebreakdown multiplication processes are reported. The existence of prebreakdown light emission near the anode is reported in paper [13]. This light emission is explains as the influence of previous discharge. In paper [14], it is reported that the prebreakdown light emission is affected by the corona appearance on the rod-shaped anode.

Electrical Breakdown Voltage distributions

When the applying voltage on the diode is rising linearly with the increasing rate k ($k = \mathrm{d}U/\mathrm{d}t$) the breakdown condition (1) is fulfilled at the moment when the voltage pulse reaches the value of static breakdown voltage U_S. Due to the statistical nature of the processes that lead to the breakdown [1], the breakdown voltage is of the statistical nature too and is characterized by typical breakdown distribution $f(U_B)$. Estimation of the theoretical model of the breakdown voltage distribution was a continuous research topic in the past.

One of the first models of the density distribution $f(U_B)$ neglected the breakdown formative time and considered only the influence of breakdown statistical time delay [15, 16]. In some models after that, the distribution of the breakdown voltages includes the constant value of the breakdown formative time delay [17–21]. In these models, the consequence of constant value of formative time delay is the existence of the initial voltage U_F, which appears as the shifting parameter of actual distribution. These models were able to describe the density distribution $f(U_B)$ with better accuracy, but they did not have the good agreement with the experimental data for small voltage values (the "left tail" of the distributions). This disagreement cannot be observed if the density distributions are presented with the Laue diagrams. The last can be a consequence of the neglecting the Gaussian distribution of the breakdown formative time.

The aim of this investigation is to define, experimentally and theoretically, the breakdown voltage distribution in the diode in which the positive corona appears on anode in pre-breakdown regime. When the voltage rises linearly in gas diode, the corona is only a segment in the gas breakdown process, which increases the yield in the diode gap. Estimation of the breakdown voltage distribution, presented in this paper, is based on the nonlinear increase of yield in the diode gap with the applied voltage.

2. THEORETICAL MODEL OF ELECTRICAL BREAKDOWN DENSITY DISTRIBUTIONS

The new model of breakdown voltage distribution is presented in this paper. This model is based on the convolution model of the breakdown time delay, reported in references [22–26].

In the aim better to understand the physical processes involved in the creation of shape of the breakdown voltage distribution, the theoretical model of breakdown voltage density distribution $f(U_B)$ is developed. It was done by using the convolution based time-delay statistical model which is developed and tested recently [22–26]. The values of breakdown voltages U_B (always greater than the static breakdown voltage U_S) are connected with corresponding breakdown time-delay t_D values by expression:

$$U_B = U_S + kt_D = U_S + k(t_S + t_F). \quad (2)$$

Being dependent on the stochastic variable t_D in the series of measurement, the breakdown voltage U_B occurred with the characteristic density distribution $f(U_B)$. This statistical model assumed the statistical character of the both the statistical time delay and the formative time delay, with their characteristic distributions. However, this model had to be adapted in order to be applied for the breakdown voltage distributions. Namely, the applied voltage on gas diode is not constant, but rises linearly with the constant voltage increase rate *k*, and consequently, the breakdown probability *P*, that determines statistical time delay, is not constant.

Since the conditions in the diode are changed during voltage increase (both probability and yield rise with voltage), the presumption is that the statistical time delay obeys Rayleigh distribution.

Using these presumptions and the relation between the breakdown time delay and the breakdown voltage (2), the statistical model of the breakdown voltage density distribution $f(U_B)$ is created. In particular, it should describe the ”left tail” of distribution $f(U_B)$ more accurately than the previous models. The total time delay is treated as random variable $\mathbf{t_D}$, with values t_D (*i.e.* measured values of total time delay). The random variables $\mathbf{t_D}$ is considered as the sum of two independent random variables $\mathbf{t_S}$ and $\mathbf{t_F}$ ($\mathbf{t_D} = \mathbf{t_S} + \mathbf{t_F}$).

The first random variable is the breakdown statistical time delay $\mathbf{t_S}$ (with values t_S), with the Rayleigh distribution f_S:

$$f_S = \frac{t}{C^2}\exp\left(-\frac{t^2}{2C^2}\right). \tag{3}$$

The single parameter of this distribution is *C*. The mathematical expectation $E(\mathbf{t_S})$ and standard deviation $\sigma(\mathbf{t_S})$ of this distribution are connected with parameter *C* with relations:

$$E(\mathrm{t_S}) = C\sqrt{\frac{\pi}{2}} \quad \text{and} \quad \sigma(\mathbf{t_S}) = C\sqrt{\frac{4-\pi}{2}} \tag{4}$$

Second variable is discharge formative time $\mathbf{t_F}$ (with values t_F), with Gaussian distribution f_F, given with:

$$f_F = \frac{1}{2\pi\sigma(\mathbf{t_F})}\exp\left(\frac{(t - E(\mathrm{t_F}))^2}{2\sigma(\mathbf{t_F})^2}\right). \tag{5}$$

The parameters of Gaussian distribution are the mathematical expectation $E(\mathbf{t_F})$ and standard deviation $\sigma(\mathbf{t_F})$. The expression of the density distribution of the random variable $\mathbf{t_D}$ can be obtained as the convolution of the density distributions of the random variables $\mathbf{t_S}$ and $\mathbf{t_F}$:

$$f(t_D) = \int_0^{t_D} f_S(t) f_F(t_D - t)\,\mathrm{d}t \tag{6}$$

In order to obtain the appropriate values of Rayleigh and Gaussian distribution parameters, the Monte-Carlo simulation algorithm is developed to generate the distribution of the random variable $\mathbf{t_D}$. The generator of pseudo-random numbers, subroutines for the Gaussian distribution (the Box-Muller method) and the Rayleigh distribution (the method of the inverse function) are taken from [27, 28]. The parameters of the statistical time delay and formative time distribution ($E(\mathbf{t_S})$, $E(\mathbf{t_F})$ and $\sigma(\mathbf{t_F})$) are considered as fitting parameters connected with experimental time delay mean value $\overline{t_D}$ and experimental standard deviation σ_E:

$$\begin{aligned} t_D &= E(\mathbf{t}_\mathbf{S}) + E(\mathbf{t}_\mathbf{F}), \\ \sigma_D^2 &= \sigma(\mathbf{t}_\mathbf{S})^2 + \sigma(\mathbf{t}_\mathbf{F})^2, \end{aligned} \tag{7}$$

Using the relation (2), the breakdown voltage density distribution can be described as:

$$f(U_B) = f(t_D)\frac{\mathrm{d}t_D}{\mathrm{d}U_B}. \tag{8}$$

In present estimation the breakdown voltage density distributions $f(U_B)$ are obtained by the numerical integration of equation (8) adopting the "mechanical quadrature" method [27] and using the relation (13).

The consistency of the numerically generated and experimental distributions during the Monte-Carlo simulation was checked performing the χ^2 test (see, for example, [29]). For more details about numerical procedure and distribution parameters: $E(\mathbf{t_S})$, $\sigma(\mathbf{t_S})$, $E(\mathbf{t_F})$ and $\sigma(\mathbf{t_F})$, see [22–26].

3. EXPERIMENT

A neon-filled diode with a tube volume of 300 cm^3 is used. The electrodes are different in shape. The Cu cathode is cylindrical, with a diameter of 6.5 mm and a height of 6.5 mm. The anode is a simple Mo unpolished rod with a diameter of 2 mm. The gap between the front bases of the cathode and the tip of the anode is 24 mm. The gas tube was made based on the X-ray tube standard. The tubes were baked out at 350°C and pumped down to a pressure of 10^{-7} mbar. After that, the tube was filled with Matheson research-grade neon at a pressure of 1.33 mbar.

The experimental layout is presented in Fig. 1. The shape of linearly rising voltage impulse is generated by PC. This voltage signal defined the output of the High Voltage Power Supply (Spellman MPS10P10/24). Values of the breakdown voltages are detected by digital storage oscilloscope (Tektronix TDS 2012B). These values are transferred to PC for further analyses. Each measuring series consist of 1 500 successive and independent measurements. The value of static breakdown voltage $U_S = 253.4\ \mathrm{V}$ is determined from fitting procedure of experimental data for breakdown minimal values [21].

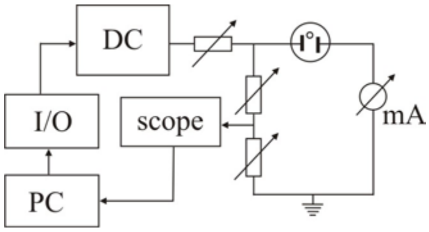

Fig. 1 – Experimental layout.

4. RESULTS

The breakdown voltage density distributions, for increasing voltage rates from 0.3 V/s to 26 kV/s, are presented in Fig. 2 and Fig. 3. The experimental breakdown voltage distributions are given by histograms, according to the criterion that in the class with maximum frequency should be around 20% of the measured values. Histograms are normalized dividing the relative frequencies of all classes by the class width ΔU_B. Each histogram is drawn on basis of 1500 successive and independent measurements of breakdown voltage.

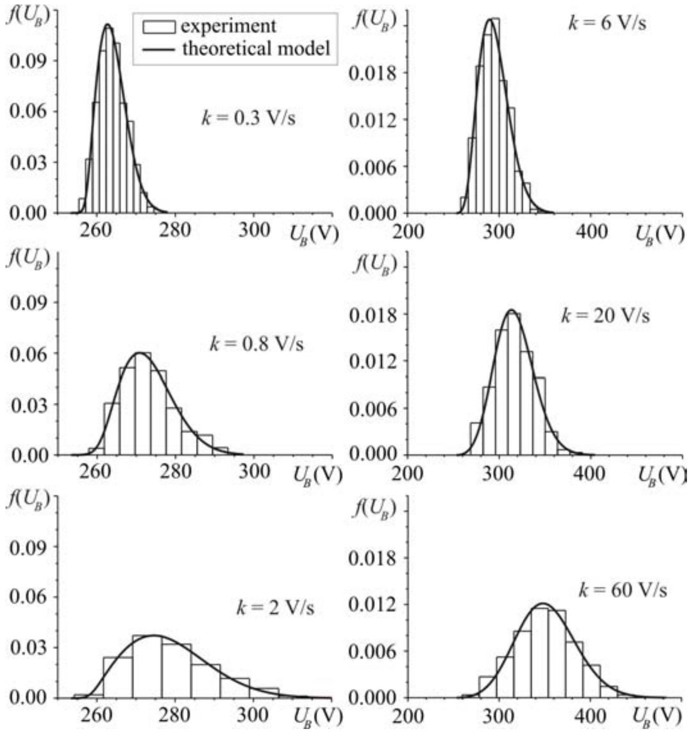

Fig. 2 – Experimental and theoretical breakdown voltage distributions for different increasing voltage rates k indicated in figure.

Obtained experimental density distributions are compared with theoretical model of electrical breakdown voltage distributions (described in Section 2). The breakdown voltage distributions based on theoretical model are presented with solid lines. The good agreement of the theoretical distributions with the experimental distribution can be seen in Fig. 2 and Fig. 3. As was expected, the distributions are wider with the increase of the *k,* and both "left" and "right tail" became significant.

The details of the theoretical model of the breakdown voltages distributions are described in Section 2. The values of the Rayleigh and Gaussian distribution parameters are obtained using the Monte Carlo simulation technique (as described in Section 2). The expected values of statistical time delay $E(\mathbf{t_S})$ and formative time delay $E(\mathbf{t_F})$, as well as, the mean values of experimentally obtained time delay are presented in Fig. 4. Good description of the "left tail" of experimentally obtained breakdown voltage distributions is consequence of the introduction of formative time delay distribution in applied statistical model.

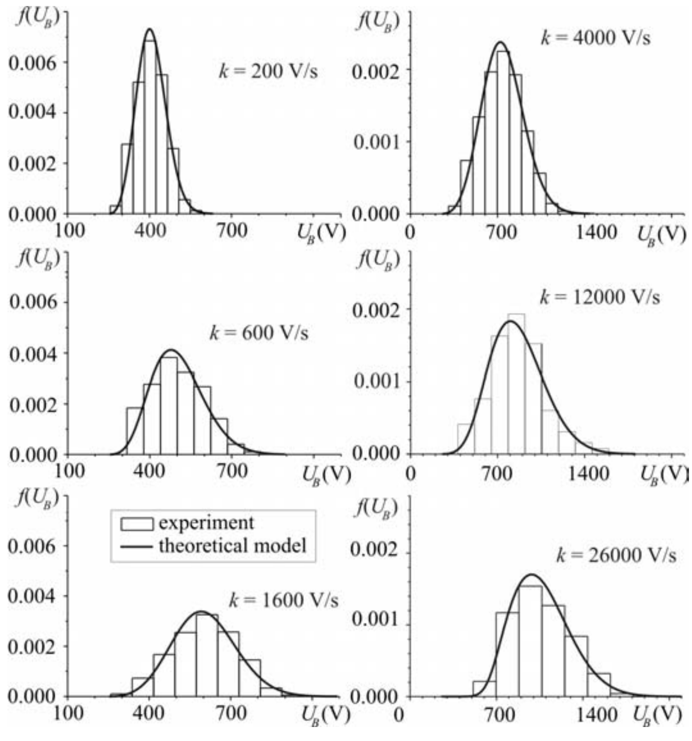

Fig. 3 – Experimental and theoretical breakdown voltage distributions for different increasing voltage rates *k* indicated in figure.

The actual values of the yield, for all used the increasing voltage rates, are represents in Fig. 5. These values correspond to the mean values of statistical time delay breakdown voltages. As can be seen from Fig. 5 agreement between values of yield estimated according to the physical and statistical model is good, which indicate the validity of applied approximations in both models. From Fig. 5 can seen that the yield grows nonlinearly with the overvoltage, which indicate that corona appearance on anode irreversibly change conditions in diode. The consequence of that is decrease of the time of initial electron appearance, *i.e.* statistical time delay t_S and the formative time delay t_F become significant.

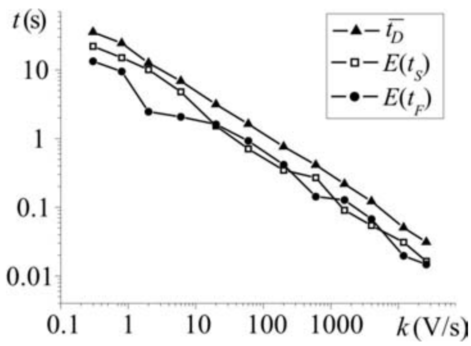

Fig. 4 – Values of $\overline{t_D}$, $E(t_S)$ and $E(t_F)$ in function of the voltage increasing rate *k*, obtained by theoretical model.

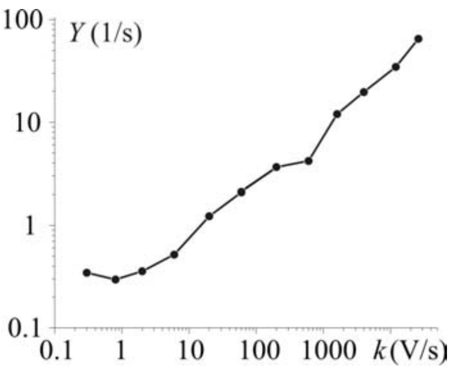

Fig. 5 – The actual values of yield *Y* in function of *k* obtained by theoretical model.

5. CONCLUSION

The electrical breakdown voltage distributions of the diode filled with Ne on 1.33 mbar pressure are presented in this paper. The anode is the unpolished wire with well defined corona appearance in prebreakdown regime. Distributions are determinated for the applied voltage increasing rates from 0.3 V/s to 26 kV/s.

The electrical breakdown voltage distributions are compared with the theoretically obtained distributions on the basis statistical convolution model. In these models the nonlinear increase of yield was estimated what agrees with the fact that corona appears on anode in the prebreakdown regime. The main contribution of this paper is the introduction of the formative time delay distribution which resulted in very good agreement between theoretically estimated and experimentally determined the breakdown distributions, especially in the most interesting region of the “left tail” of these distributions.

Acknowledgments. This work was supported by the Ministry of Education and Science of the Republic of Serbia (Project 43011 and 43012).

EFERENCES

1. J. M. Meek and J. D. Craggs, *Electrical Breakdown of Gases*, Wiley, New York, 1978.
2. M. Kristiansen and A. H. Guenther, *Plasma Applications, in Electrical Breakdown and Discharges in Gases*, Editors E. E. Kunhart and L. H. Luessen, Plenum, New York, 1983.
3. B. Lončar, P. Osmokrović, and S. Stanković, IEEE Trans. Nucl. Sci., **76**, 1725–1731 (2003).
4. M. M. Gutorov, *Basics of Light Technics and Light Sources* (in Russian), Energoatomizdat, Moscow, Russia, 1983.
5. K. Zuber, Annu. Phys., **76**, 231 (1925).
6. M. von Laue, Annu. Phys., **76**, 261–265 (1925).
7. L. B. Loeb, Rev. Mod. Phys., **20**, 151 (1948).
8. R. A. Wijsman, Phys. Rev., **75**, 833–838 (1949).
9. F. Llewellyn-Jones, *The Development of Theories of the Electrical Breakdown of Gases, in Electrical Breakdown and Discharges in Gases*, Editors E. E. Kunhart and L. H. Luessen, Plenum, New York, 1983.
10. M. Zambra, M. Favre, J. Moreno, H. Chuaqui, E. Wyndham, and P. Choi, IEEE Trans.Plasma Sci., **27**, 746–751 (1999).
11. J. Moreno, M. Zambra, and M. Favre, IEEE Trans. Plasma Sci., **30**, 417–422 (2002).
12. R. S. Moss, J. G. Eden, and M. J. Kushner, J. Phys. D, Appl. Phys., **37**, 2502–2509 (2004).
13. E. Wagenaars, M. D. Bowden, and G. M. W. Kroesen, Plasma Sources. Sci. Technol., **14**, 342–350 (2005).
14. M. K. Radović, Č. A. Maluckov, S. A. Rančev, IEEE Trans. Plasma Sci., **35**, 1738–1742 (2007).
15. M. Radović, M. Pejović, and Đ. A. Bošan, *Contrib. Papers of the 13th Int. Symp. on the Phys. on Ionized Gases, Sibenik*, Editor M. V. Kurepa, Univ. Belgrade, Belgrade, Yugoslavis, 1986, pp. 439–442.
16. M. M. Pejović and R. D. Filipović, Int. J. Electron., **20**, 251–256 (1989).
17. M. Radović, T. Jovanović, Č. Maluckov, and O. Stepanović, Balkan Phys. Lett., **5**, 1447–1450 (1997).
18. M. Pejović, G. S. Ristić, and J. P. Karamarković, J. Phys. D, Appl. Phys., **35**, R. 91–R. 103 (2002).
19. M. Radović and Č. Maluckov, IEEE Trans. Plasma Sci., **29**, 832–836 (2001).
20. Č. A. Maluckov and M. K. Radović, Contrib. Plasma Physics, **42**, 556-568 (2002).
21. Č. A. Maluckov and M. K. Radović, IEEE Trans. Plasma Sci., **30**, 1579–1601 (2002).
22. Č. A. Maluckov, J. P. Karamarković, and M. K. Radović, IEEE Trans. Plasma Sci., **31**, 1344–1348 (2003).
23. Č. A. Maluckov, J. P. Karamarković, M. K. Radović, and M. M. Pejović, Phys. Plasmas, **11**, 5328–5334 (2004).
24. Č. A. Maluckov, J. P. Karamarković and M. K. Radović, Contrib. Plasma Physics, **45**, 118–129 (2005).
25. Č. A. Maluckov, J. P. Karamarković, M. K. Radović and M. M. Pejović, IEEE Trans. Plasma Sci., **34**, 2–6 (2006).
26. Č. A. Maluckov, J. P. Karamarković, M. K. Radović and M. M. Pejović, Phys. Plasmas, **13**, 083502 (2006).
27. D. E. Knuth, *Seminumerical Algorithms*, Second Edition (*2. The Art of Computer Programming*), Addison-Wesley, Reading, MA, 1981.
28. W. H. Press, S. A. Teukolsky, W. T. Vetterling, and B. P. Flannerly, *Numerical Recipes in Fortran 77: The Art of Scientific Computing,* Cambridge Univ. Press, Cambridge, U.K., 1997. (2nd ed., 1 of *Fortran Numerical Recipes*).
29. D. D. Wackerly, W. Mendenhall III, and R. L. Scheaffer, *Mathematical Statistics with Applications*, Duxbury, Belmont, 1996, pp. 663–668.